OVERSAMPLING COMPLEX-MODULATED DIGITAL FILTER BANK PAIRS SUITABLE FOR EXTENSIVE SUBBAND-SIGNAL AMPLIFICATION

Thomas Kurbiel, Heinz G. Göckler and Daniel Alfsmann

Digital Signal Processing Group (DISPO), Ruhr-Universität Bochum, 44780 Bochum, Germany
phone: +49 234 32 22873, fax: +49 234 32 02873, email: kurbiel@nt.rub.de, web: www.dsv.rub.de

ABSTRACT

Oversampling, complex-modulated digital subband coder filter banks are commonly adopted in modern hearing aids to allow for individual amplification of subband signals in order to compensate for hearing losses of impaired persons. Minimum power consumption and low group delay have been the main concern in the design of these filter banks. Guaranteeing frequency-independent and low group delay in case of subband-signal amplification has, however, been neglected in the past.

In this contribution, we investigate the delay and amplification properties of oversampling complex-modulated FIR filter banks in case of extensive subband signal amplification. Based on these results, a sufficient condition for constant group delay is derived. Furthermore, we present a compensation method which allows for constant group delay, even if the sufficient condition is violated. An illustrative design example demonstrates the potential of the compensation method.

1. INTRODUCTION

Primal task of hearing aids is to amplify the microphone signal in a frequency-selective manner in order to compensate for the hearing loss of an impaired person. In addition to this task present-day hearing aids provide a vast spectrum of frequency-band-dependent processing steps, such as noise reduction and speech enhancement [4]. For this purpose we use filter banks pairs (FBP), which first decompose the microphone signal by an analysis filter bank (AFB) into several subband-signals at an adequately reduced sampling rate, and then reconstruct the manipulated subband-signals by a synthesis filter bank (SFB). Due to low battery energy available in hearing aids, non-uniform filter banks with frequency-dependent filter bandwidths at Bark scale intervals [11] are presently disregarded and reserved for future research. Currently, the energy constraints are accounted for best dealt with by use of uniform, oversampling, complex-modulated (DFT) polyphase filter banks applying FIR filters that essentially avoid aliasing and imaging disturbance by sufficiently high stopband attenuation of the prototype filters [10, 9, 3]. Another challenge of similar importance in hearing aids is the overall signal delay of the cascade of the AFB and the SFB. The total delay (including subband-signal manipulation) of the filter bank must not exceed 5...8ms [8], since otherwise the signal quality degrades as a result of the superposition of the direct and the processed (delayed) sound signal in the auditory canal. In addition to this requirement, the delay must approximately be constant versus frequency even in any case of extensive subband-signal amplification. The demand for a low signal delay of the cascade of the AFB and the SFB is equivalent to the requirement for a low group delay of both the analysis and synthesis prototype filters. Therefore the lowest possible signal delay is obtained by using non linear-phase (LP) FIR prototype filters.

In the past, many attempts have been made to design oversampling, complex-modulated filter bank prototype filter pairs with approximately constant group delay that, at the same time, do not exceed a prescribed value. In [2], an iterative method has been proposed, which allows for controlling the distortion level for each frequency component and directly minimizes subband-aliasing and imaging. In a similar design approach [7], non-linear aliasing and
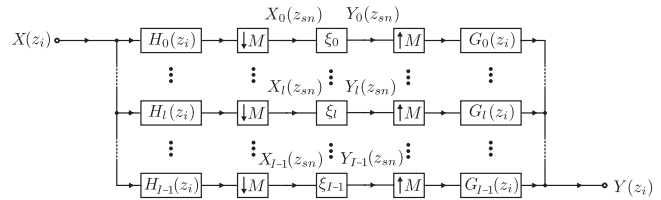

Figure 1: Uniform Oversampling filter bank pair, oversampling factor $\mathscr{O} = I/M \in \mathbb{N}$

imaging disturbance is minimised by alternatingly optimising the AFB and SFB prototype filters, respectively. The design methodology according to [1, 5] aims at an optimum FBP output SNR for arbitrary subband-signal amplification in conjunction with low and flat overall group delay.

It has been observed that extensive subband-signal amplification in complex-modulated FBP gives rise to severe group delay and amplification distortions especially at the interception of contiguous subbands with different amplification. To this end, subsequently we investigate the properties of oversampling complex-modulated FIR FBP for differing amplification of the subband-signal. From these results we derive a sufficient condition for the absence of these undesired distortions. Finally, a compensation method is proposed to meet this sufficient condition for a wide variety of oversampling complex-modulated FBP designs. Illustrative examples are used troughout.

2. OVERSAMPLING COMPLEX-MODULATED FIR FILTER BANK PAIRS

For a uniform oversampling complex-modulated I-channel filter bank with additional subband signal amplification $\xi_l, \forall l = 0, \ldots, I-1$, as shown in Fig. 1, the AFB und SFB filters, respectively, are derived from common prototype filters by modulation [9, 3]:

$$H_l(z_i) = H\left(z_i W_I^l\right), l = 0, \ldots, I-1 \quad (1)$$

$$G_l(z_i) = G\left(z_i W_I^l\right), l = 0, \ldots, I-1 \quad (2)$$

The input signal $x(n) \xleftrightarrow{z\mathrm{T}} X(z_i)$ in Fig. 1 is simultaneously passed through all AFB channel filters $H_l(z_i)$, $l = 0, \ldots, I-1$ and subsequently downsampled by a factor of M, yielding the subband signal representation:

$$X_l(z_{\mathrm{sn}}) = \frac{1}{M} \sum_{k=0}^{M-1} H_l\left(z_{\mathrm{sn}}^{1/M} W_M^k\right) X\left(z_{\mathrm{sn}}^{1/M} W_M^k\right), l = 0, 1, \ldots, I-1, \quad (3)$$

where use is made of the alias component representation [9, 3], and $W_M = \mathrm{e}^{-\mathrm{j}2\pi/M}$. Next, each subband signal is individually amplified by the factor $\xi_l, l = 0, \ldots, I-1$, yielding

$$Y_l(z_{sn}) = \xi_l \cdot X_l(z_{sn}), l = 0, 1, \ldots, I-1 \quad (4)$$

In the SFB, the amplified and M-fold upsampled subband-signals $Y_l(z_i^M) = Y_l(z_{sn})$ are combined to form the z-domain output signal representation [3]:

$$Y(z_i) = \sum_{l=0}^{I-1} G_l(z_i) Y_l(z_i^M) \tag{5}$$

Inserting the upsampled form of (3) into (5), we obtain:

$$
\begin{aligned}
Y(z_i) &= \sum_{l=0}^{I-1} G_l(z_i)\,\xi_l \left[\frac{1}{M} \sum_{k=0}^{M-1} H_l\left(z_i W_M^k\right) X\left(z_i W_M^k\right) \right] \\
&= \frac{1}{M} \sum_{k=0}^{M-1} X\left(z_i W_M^k\right) \left[\sum_{l=0}^{I-1} \xi_l H_l\left(z_i W_M^k\right) G_l(z_i) \right]
\end{aligned} \tag{6}
$$

Obviously, the output signal representation $Y(z_i)$ depends on all M modulation components $X(z_i W_M^k), k = 0,\ldots,M-1$, of the input signal. All these components are filtered by the compound term $\sum_{l=0}^{I-1} \xi_l H_l(z_i W_M^k) G_l(z_i)$ before combination. The transfer function of the zeroth ($k = 0$) modulation component is considered as the distortion function [9, 3]:

$$F_{dist}(z_i) = \frac{1}{M}\left[\sum_{l=0}^{I-1} \xi_l H_l(z_i) G_l(z_i) \right]. \tag{7}$$

Particularly in our considerations, this distortion function determines the properties of the filter bank almost exclusively, since aliasing and imaging are assumed to be negligible as a result of sufficiently high AFB and SFB prototype filter stopband attenuation [1, 5]. Inserting (1) and (2) into (7), we obtain

$$F_{dist}(z_i) = \frac{1}{M}\left[\sum_{l=0}^{I-1} \xi_l H\left(z_i W_I^l\right) G\left(z_i W_I^l\right) \right]. \tag{8}$$

Desired Characteristics

In order to measure the quality of any actual FBP distortion function, we define a *desired* distortion function in polar coordinate representation as follows:

$$
F_{dist}^{des}\left(e^{j\Omega}, \xi_0,\ldots,\xi_{I-1}\right) = \\
\left| F_{dist}^{dist}\left(e^{j\Omega}, \xi_0,\ldots,\xi_{I-1}\right) \right| \cdot e^{-j\cdot\Omega\cdot\tau_g^{des}} \tag{9}
$$

The magnitude of (9) reflects the amplification pattern applied to the subband signals, where $|F_{dist}^{des}(e^{j\Omega},\xi_0,\ldots,\xi_{I-1})|$ is unity (allpass function) for $\xi_l = 1, \forall l = 0,\ldots,I-1$. The linear-phase term of (9) defines the requirement that the constant group delay τ_g^{des} shall be independent of the amplification pattern $\xi_l, l = 0,\ldots,I-1$. Since the FBP must transfer all spectral components of the input signal $x(n) \longleftrightarrow X(z_i)$ subject to frequency-selective amplification [1], it follows that $|F_{dist}^{des}(e^{j\Omega},\xi_0,\ldots,\xi_{I-1})| > 0\ \forall\Omega$ and, hence, the distortion function (8) has no zero on the z-plane unit circle [6]. As a consequence, the above definition of the desired distortion function (9) corresponds to the frequency response of a linear-phase FIR filter, where the magnitude of (9) can be interpreted as the associated zero-phase response [6]. In fact, the actual overall FBP transfer function has to approximate the desired distortion function (9). In case of $\xi_l = 1, \forall l$, the desired response (9) represents a linear-phase allpass function.

3. THE IMPACT OF AMPLIFICATION

To begin with, we examine the impact of subband signal amplification on the group delay of the distortion function. For demonstration purposes we choose a realistic uniform oversampling complex-modulated I-channel filter bank, where $I = 64$ and $M = 16$. Hence,
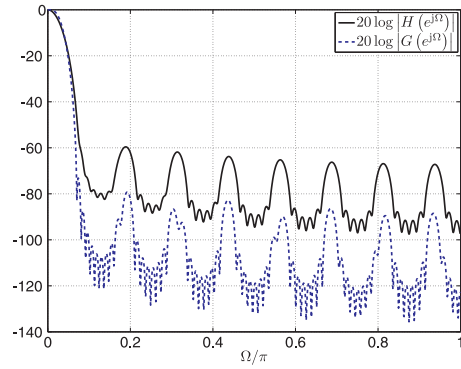
(a) Log Magnitude
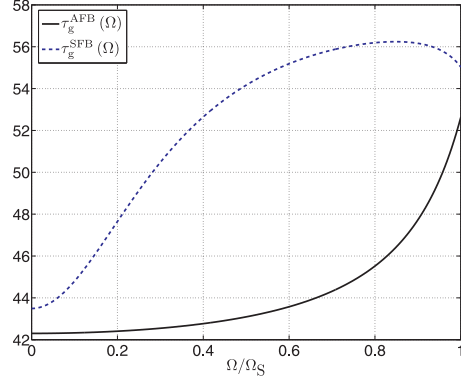
(b) Group Delay

Figure 2: FBP prototype filters

the oversampling factor $\mathcal{O} = I/M = 4$. The passband and stopband edge frequencies of the corresponding filter bank prototype filters are $\Omega_p = \pi/64$ and $\Omega_s = \pi/16$, respectively [1]. The prototype filter lengths of the AFB and SFB are $N_h = 80$ and $N_g = 120$, respectively. The prototype filters are designed according to [7]. Both filters are matched such that the distortion function of an oversampling I-channel complex-modulated FIR filterbank approximates a constant delay of $\tau_g = I = 64$ [5], and the non-linear disturbance (aliasing & imaging) is minimized. Fig. 2 (a) shows the logarithmic magnitude responses of the AFB and SFB prototype filters. The characteristics of the stopband responses are typical for oversampling FBPs with minimised disturbance [7, 2]. Fig. 2 (b) depicts the group delay of the prototype filters both in the passband and the transition band. Obviously, both filters do not even approximately possess the linear-phase property. The mean values of the group delay within passband and transition bands, which are needed for a system modelling later on, are $\overline{\tau}_{g,AFB} = 44.11$ and $\overline{\tau}_{g,SFB} = 52.25$, respectively.

Next, an amplification pattern $\xi_l, \forall l = 0,\ldots,I-1$, for the subband channels is implemented:

$$
\begin{aligned}
\xi_l &= 50 &\triangleq 34\,\text{dB}, \forall l = 12,\ldots,19 \\
\xi_l &= 300 \triangleq 49.5\,\text{dB}, \forall l = 20,\ldots,27 \\
\xi_l &= 15 &\triangleq 23\ \text{dB}, \forall l = 28,\ldots,35
\end{aligned} \tag{10}
$$

For the remaining channels we assume $\xi_l = 1$. Fig. 3 (a) shows the magnitude response of the distortion function with the above subband-signal amplification. What strikes most are the huge peaks, which appear only at the interceptions between two contiguous channels with different amplifications ξ_l, e.g. between channel $l = 19$ and $l = 20$. Their heights depend on the ratio of amplifications of contiguous channels. The smallest peak is observed at

(a) Magnitude Response
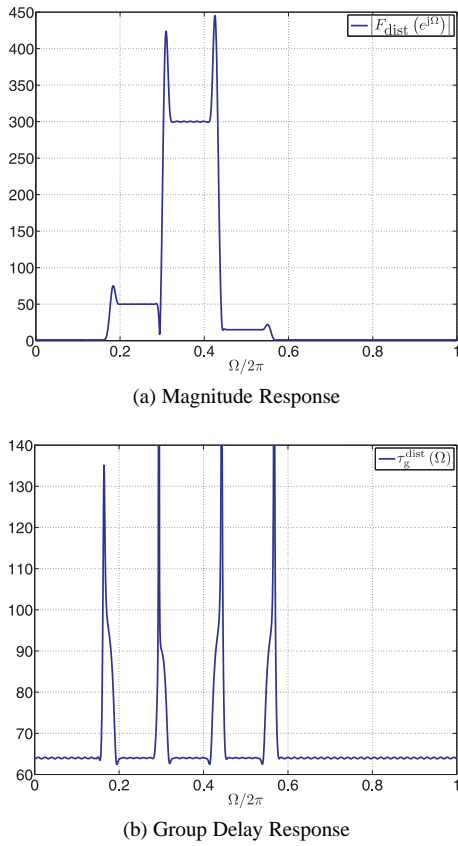

(b) Group Delay Response

Figure 3: Dist. func. with subband-signal amplification

the transition between channel 35 and 36, since the amplification ratio is only 15. The corresponding group delay response in Fig. 3 (b) also exhibits high peaks at the transitions of amplifications. The peaks extend over two channels and their maximum value is increased by more than two-fold compared to the mean value of $\tau_\mathrm{g} = I = 64$. Except for these transitions, the group delay behaves the way it is expected of an oversampling complex-modulated filterbank [5].

Based on these results, we observe that oversampling complex-modulated filterbanks do not inherently guarantee approximately constant group delay, when different amplifications of the subband signals are applied. In the following we first examine the reason for this effect and, based on the obtained insight to cancel the undesired distortions.

3.1 Linear-Phase Approximation Model

In order to understand the mechanism responsible for the effects described above, we make some simplifying approximations concerning the prototype filters. An example will show that these approximations are sufficiently correct for our considerations.

The first approximation made concerns the AFB prototype filter. Despite the fact, that the group delay is highly non-constant, as to be seen in Fig. 2 (b), we yet assume the prototype filter to have an overall constant group delay of $\overline{\tau}_{g,\mathrm{AFB}} = 44.11$, read from Fig. 2 (b). Using this approximation, we model the AFB prototype filter as a linear-phase filter:

$$H\left(\mathrm{e}^{\mathrm{j}\Omega}\right) \approx H_0\left(\mathrm{e}^{\mathrm{j}\Omega}\right) \cdot \mathrm{e}^{-\mathrm{j}\overline{\tau}_{g,\mathrm{AFB}}\cdot\Omega} \tag{11}$$

where $H_0\left(\mathrm{e}^{\mathrm{j}\Omega}\right)$ represents the zero-phase response and $\overline{\tau}_{g,\mathrm{AFB}}\cdot\Omega$ the linear-phase. The SFB FIR prototype filter is modelled in the same manner:

$$G\left(\mathrm{e}^{\mathrm{j}\Omega}\right) \approx G_0\left(\mathrm{e}^{\mathrm{j}\Omega}\right) \cdot \mathrm{e}^{-\mathrm{j}\overline{\tau}_{g,\mathrm{SFB}}\cdot\Omega} \tag{12}$$

where $\overline{\tau}_{g,\mathrm{SFB}} = 52.25$.

Next, we have to show that the above model approximations are sufficiently exact for our purposes. To this end, we replace the original nonlinear-phase FIR prototype filters according to Fig. 2 in the actual distortion function (8) with linear-phase filters (11) and (12) of suitable lengths. Using the relation between group delay and filter length $\tau_\mathrm{g} = (N-1)/2$ of linear-phase FIR filters [6], the lengths of the model filters (11) and (12) are chosen such that their group delays approximate the mean values of the group delays of the respective filters of Fig.2, $\overline{\tau}_{g,\mathrm{AFB}} = 44.11$ and $\overline{\tau}_{g,\mathrm{SFB}} = 52.25$. With the corresponding closest (rounded) integer group delays, the model filter lengths are readily derived: $N_\mathrm{h} = 89$ and $N_\mathrm{g} = 105$.

With these linear-phase model filters, the original FBP is re-designed by using a modified version of the design algorithm [7] being adapted to the design of FBP with linear-phase filters. Since the overall expenditure of the linear-phase design is smaller and, in addition, due to the linear-phase constraint, the approximation with the linear-phase model filters is worse than that with the original filters according to Fig. 2: The peak-to-peak deviation from the allpass distortion function is 0.17dB rather than 0.03dB, and the minimum stopband attenuations are considerably lower than those of Fig. 3 (a). Nevertheless, the approximation of the desired distortion function is good enough, and the impact of nonlinear disturbance due to aliasing and imaging is still negligible. By again using the amplification pattern (10), the magnitude response of the distortion function of the linear-phase model FBP is depicted in Fig. 4 (a). As it is obvious from a comparison of Figs. 3 (a) and 4 (a), the impact of amplification is reasonably well approximated by the model FBP. Only at the interceptions of different amplification factors ξ_l, the model FBP exhibits slightly higher overshoots. The corresponding group delay behaviour of the model FBP distortion function is presented in Fig. 4 (b). Again, the similarity with the original nonlinear-phase design of Fig. 3 (b) is remarkable. The main group delay deviation from that of the original FBP is observed in those regions, where the amplification factors ξ_l are constant, i.e. between interceptions of different amplification factors. This increased group delay deviation from the expected mean value of $\tau_\mathrm{g} = I = 64$ gives also rise to slightly higher deviations of the magnitude of the distortion function from the desired function (9) in these regions, as deduced from a comparison of Figs. 3 (a) and 4 (a). From the above comparisons it is concluded that the model approximation (11) and (12) is justified. Hence, we use this model for the following investigations.

3.2 A Sufficient Condition

Next, we use the above linear-phase model to identify the origin for the observed effects presented at the beginning of this section. To this end, both approximations (11) and (12) are introduced into the distortion function (8), and the result is compared with (9). We use the subsequent abbreviation: $\overline{\tau}_\Sigma = \overline{\tau}_{g,\mathrm{AFB}} + \overline{\tau}_{g,\mathrm{SFB}}$. To begin with, we examine the product of the AFB and SFB prototype filter transfer functions of the approximations (11) and (12):

$$H\left(z_\mathrm{i}\right) \cdot G\left(z_i\right) \approx H_0\left(z_\mathrm{i}\right) \cdot G_0\left(z_\mathrm{i}\right) \cdot z_\mathrm{i}^{-\overline{\tau}_\Sigma}. \tag{13}$$

The aliasing components of this expression are:

$$H\left(z_\mathrm{i}W_I^l\right) \cdot G\left(z_\mathrm{i}W_I^l\right) \approx \tag{14}$$

$$W_I^{-l\cdot\overline{\tau}_\Sigma} \cdot H_0\left(z_\mathrm{i}W_I^l\right) \cdot G_0\left(z_\mathrm{i}W_I^l\right) \cdot z_\mathrm{i}^{-\overline{\tau}_\Sigma} \tag{15}$$

Inserting (14) into the distortion function (8), we obtain:

$$F_\mathrm{dist}\left(z_\mathrm{i}\right) \approx$$

$$z_\mathrm{i}^{-\overline{\tau}_\Sigma} \cdot \left[\frac{1}{M}\sum_{l=0}^{I-1}\xi_l \cdot W_I^{-l\cdot\overline{\tau}_\Sigma} \cdot H_0\left(z_\mathrm{i}W_I^l\right) \cdot G_0\left(z_\mathrm{i}W_I^l\right)\right] \tag{16}$$

(a) Magnitude Response
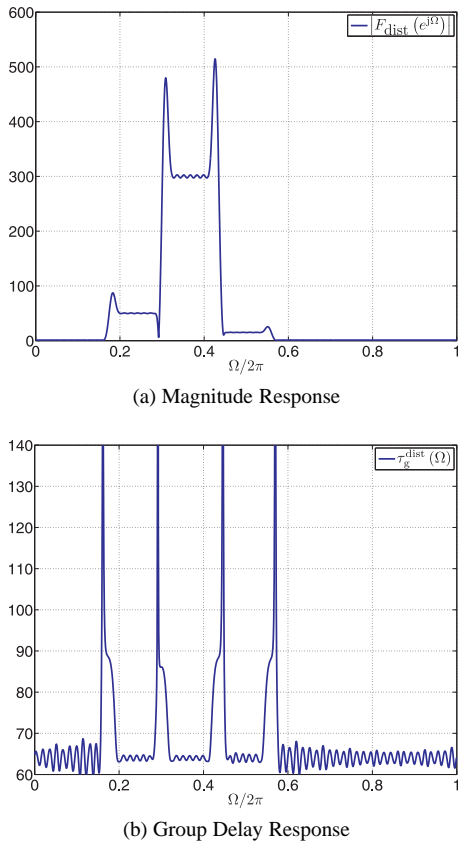

(b) Group Delay Response

Figure 4: Dist. func. with amplification based on linear-phase filters

This expression formally resembles condition (9). It can be split up in an amplification-independent delay term and an amplification-dependent magnitude term (term within brackets). Comparing (16) with (9), the magnitude term of (16) should be real-valued which, in general, is not satisfied due to the complex factors $W_I^{-l \cdot \overline{\tau}_\Sigma}$ of (16). Nevertheless, we can derive a sufficient condition for a constant group delay of complex-modulated filter banks by requiring:

$$W_I^{-l \cdot \overline{\tau}_\Sigma} = e^{jl \cdot \overline{\tau}_\Sigma \cdot 2\pi/I} = 1, \quad \forall l = 0, \dots, I-1 \qquad (17)$$

Condition (17) is satisfied by

$$\overline{\tau}_\Sigma \cdot 2\pi/I = \left(\overline{\tau}_{g,\text{AFB}} + \overline{\tau}_{g,\text{SFB}} \right) \cdot 2\pi/I = \kappa \cdot 2\pi$$
$$\overline{\tau}_{g,\text{AFB}} + \overline{\tau}_{g,\text{SFB}} = \kappa \cdot I, \quad \forall \kappa \in \mathbb{Z} \qquad (18)$$

This condition is likewise expressed by applying the modulo operation in the following way:

$$r = \left(\overline{\tau}_{g,\text{AFB}} + \overline{\tau}_{g,\text{SFB}} \right)_I = 0. \qquad (19)$$

When applied to the prototype filters of Fig. 2, we obtain $r = (44.11 + 52.25)_{64} = 32.36 \neq 0$. Hence, the sufficient condition (19) is violated resulting in the observed effects.

It should be noted that factor r can be considered as a quality criterion for the ability of an oversampling complex-modulated filter bank to provide constant group delay in case of subband channels amplification: The greater the factor r the worse the behaviour subject to subband signal amplification.

3.3 Compensation Approach

Fot the case the sufficient condition (19) is violated, a simple compensation method is developed which provides constant group delay of the distortion function under any amplification pattern. By using

the definition of the modulo operator, we can reformulate expression (19) as follows: $\overline{\tau}_\Sigma = r + \kappa I$, $\kappa \in \mathbb{Z}$. Introducing this form into (16), we obtain the model distortion function in dependence of factor r defined in (19):

$$F_{\text{dist}}(z_i) \approx$$
$$z_i^{-\overline{\tau}_\Sigma} \cdot \left[\frac{1}{M} \sum_{l=0}^{I-1} \xi_l \cdot W_I^{-l \cdot r} \cdot H_0\left(z_i W_I^l\right) \cdot G_0\left(z_i W_I^l\right) \right]. \qquad (20)$$

The above necessary condition (19) is obviously met if the real amplification factors $\check{\xi}_l$ are replaced with the complex amplification factors:

$$\underline{\xi}_l = \xi_l \cdot W_I^{lr}, \, l = 0, \dots, I-1 \qquad (21)$$

which, in addition to the amplification factor ξ_l, comprise an individual complex compensation factor in each channel. The resulting distortion function is given by:

$$F_{\text{dist}}(z_i) \quad \approx$$
$$z_i^{-(\overline{\tau}_{g,\text{AFB}} + \overline{\tau}_{g,\text{SFB}})} \cdot \left[\frac{1}{M} \sum_{l=0}^{I-1} \xi_l \cdot H_0\left(z_i W_I^l\right) \cdot G_0\left(z_i W_I^l\right) \right], \qquad (22)$$

which satisfies condition (9) and, hence, guarantees constant group delay independently of the amplification pattern. Moreover, it should be noted that the resulting constant value of the group delay according to (22) is no longer restricted to a multiple integer of the number of channels I, as shown in [5]. Instead, the summation of the mean group delays of the prototype filters determines the overall delay.

3.4 Example

Subsequently, we apply the above compensation method to the prototype filter pair of Fig. 2. Rather than $r = 32.26$, for the complex-valued amplification factors (21) we apply the closest integer value $r = 32$. Again, the real amplification pattern used is defined by (10).

Fig. 5 depicts the magnitude and group delay responses of the distortion function. Evidently, all original artifacts of Figs. 3 and 4 are compensated. We observe an approximately constant group delay about a mean value of $\overline{\tau}_\Sigma = 44.11 + 52.25 \approx 96$. The observed peaks at the transitions in Fig. 5 (b) can be neglected, since they do not exceed 8% of the mean value.

4. CONCLUSION

We have investigated the impact of arbitrarily different amplifications of the subband signals of oversampling uniform complex-modulated filter bank pairs (FBP of the SBC-type) on their transfer characteristics, in particular, with focus on the group delay response of the FBP distortion function. First, for this class of FBP, it has been shown that extensive subband signal amplifications, in general, give rise to more or less extremal deviations from the desired *constant* group delay of the overall FBP transfer characteristic. Next, we have derived a sufficient condition for the absence of these adverse, unacceptable group delay deteriorations. Yet, most interestingly, this sufficient condition can be satisfied with particular choices of the filter lengths of the FIR prototype filters. Finally, we have proposed a compensation method which satisfies the sufficient condition for any FIR prototype filter lengths. This compensation approach merely requires to replace the real amplification factors ξ_l with complex-valued amplification factors $\underline{\xi}_l$, where $|\underline{\xi}_l| = \xi_l$. As a result, the number of multiplications for amplification is merely doubled, since the subband signals of complex-modulated FBP are complex-valued.

The main result of this study is that oversampling complex-modulated FBP applying our compensation method can unrestrictedly be used for any subband signal amplification pattern (i.e., also for hearing aids). As a consequence, the resulting *constant* FBP
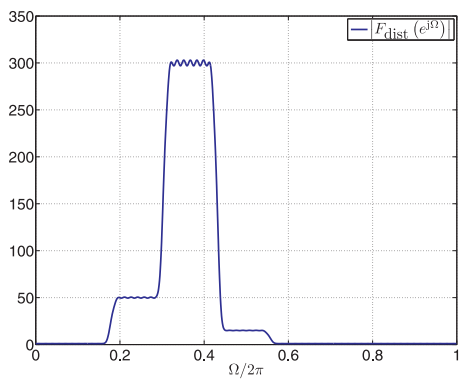
(a) Magnitude Response
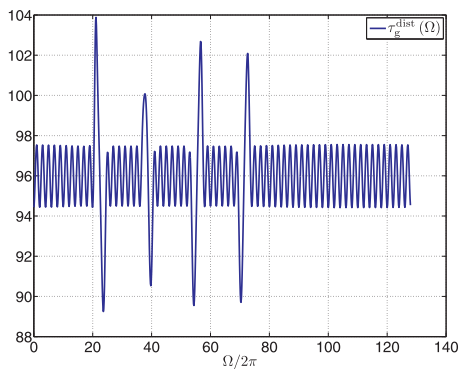
(b) Group Delay Response

Figure 5: Dist. func. with compensation approach

group delay is no longer restricted to an integer multiple of the number I of filter bank channels [5]. It is, however, slightly increased to the summation of the mean group delays of the AFB and SFB prototype filters. Nevertheless, the tight FBP group delay constraints of hearing aids can still be maintained, since our FBP designs [5, 7] generate low-delay FIR prototype filter.

In future research, we will investigate the impact of our compensation method on the signal-to-distortion ratio at the FBP output port. Especially, we are interested in the potential of noise shaping of this compensation approach.

REFERENCES

[1] D. Alfsmann, H. G. Göckler, and T. Kurbiel. Frequency domain constraints to oversampling filter bank systems in hearing aids to ensure a prescribed output signal-to-distortion ratio. *J. Advances Sign. Process.*, accepted for public., 2009.

[2] H. H. Dam, S. Nordholm, A. Cantoni, and J. M. de Haan. Iterative method for the design of DFT filter bank. *IEEE Transactions on Circuits and Systems*, 51(11):581–586, Nov. 2004.

[3] H. G. Göckler and A. Groth. *Multiratensysteme*. Schlembach Fachverlag, Willburgstetten, 2004.

[4] V. Hamacher, J. Chalupper, J. Eggers, E. Fischer, U. Kornagel, H. Puder, and U. Rass. Signal processing in high-end hearing aids: State of the art, challenges, and future trends. *J. Applied Signal Process.*, 18:2915–2929, 2005.

[5] T. Kurbiel, H. G. Göckler, and D. Alfsmann. A novel approach to the design of oversampling low-delay complex-modulated filter bank pairs. *J. Advances Sign. Process.*, accepted for public., 2009.

[6] A. V. Oppenheim and R. W. Schafer. *Discrete-Time Signal Processing*. Prentice-Hall International, London, 1989.

[7] Ch. Stöcker, Th. Kurbiel, D. Alfsmann, and H. G. Göckler. A novel approach to the design of oversampling complex-modulated digital filter banks. *Proc. Eurasip 17th European Signal Processing Conference (EUSIPCO 2009), Glasgow, Scotland*, 2009.

[8] M. A. Stone and B. C. J. Moore. Tolerable hearing aid delays. III. Effects on speech production and perception of across-frequency variation in delay. *Ear & Hearing*, 24:175–183, April 2003.

[9] P. P. Vaidyanathan. *Multirate Systems and Filter Banks*. Prentice Hall, Englewood Cliffs, NJ, 1993.

[10] P. Vary. *Ein Beitrag zur Kurzzeitspektralanalyse mit digitalen Systemen*. PhD thesis, Universität Erlangen-Nürnberg, Erlangen, Germany, 1978.

[11] E. Zwicker and H. Fastl. *Psychoacoustics: Facts and Models*. Springer-Verlag, Berlin, 1999.